Offline-Online Design for Energy-Efficient IRS-Aided UAV Communications

Tianhao Wang, Xiaowei Pang, Mingqian Liu, *Member, IEEE,* Nan Zhao, *Senior Member, IEEE,*
Arumugam Nallanathan, *Fellow, IEEE,* and Xianbin Wang, *Fellow, IEEE*

Abstract—In this correspondence, we consider the intelligent reflecting surface (IRS) assisted unmanned aerial vehicle (UAV) uplink transmission, where a UAV collects data from ground users via an IRS. The objective is to maximize the energy efficiency (EE) by jointly optimizing the UAV trajectory, user scheduling and IRS phase shifts. Unlike existing offline designs, we propose a hybrid offline-online scheme to further improve the performance with both the statistical and instantaneous channel state information (CSI). Specifically, the UAV trajectory and user scheduling are optimized based on the statistical CSI in the offline phase, followed by the online phase in which the phase shifts are readjusted based on the instantaneous CSI. Simulation results show the EE gain of the offline-online design over benchmarks.

Index Terms—Intelligent reflecting surface, unmanned aerial vehicle, statistical and instantaneous CSI, offline-online design.

I. Introduction

Unmanned aerial vehicles (UAVs) have attracted extensive attention in serving as low-altitude communication platforms, owing to their high mobility and low cost [1]. In particular, UAV can establish nearly line-of-sight (LoS) links with ground users, thereby achieving reliable transmission. Despite these advantages, the limited on-board energy greatly restrains its performance. Thus, energy efficiency (EE) is of vital importance for UAV communications [2]. In [3], the propulsion energy model of rotary-wing UAV was derived by Zeng *et al.*. Based on [3], Duo *et al.* proposed a full-duplex UAV secrecy communication scheme to maximize the EE in [4].

Recently, intelligent reflecting surface (IRS) has become a promising technology for future networks, due to its ability of reconfiguring the propagation environment [5]. By adjusting the phase shifts of all passive reflecting elements, an IRS can enhance the strength of reflected signal in the desired direction and suppress the interference with minimal power consumption. Introducing IRS into UAV has many promising advantages, such as extending the wireless coverage and improving the EE [6], [7]. Pang *et al.* in [8] discussed the typical cases of combining UAV and IRS. Zhai *et al.* studied the UAV-mounted IRS in mobile edge computing to maximize the EE in [9]. In [10], Li *et al.* studied the robust secure communications, aiming at integrating IRS and UAV in both downlink and uplink to maximize the secrecy rate. In [11], the weighted sum bit error rate (BER) and fairness BER were minimized by Hua *et al.* based on the statistical channel state information (CSI) via the joint design of UAV trajectory, IRS reflection matrix and scheduling. IRS-enhanced multi-UAV NOMA networks were investigated by Mu *et al.* in [12] to maximize the sum rate. In [13], Misbah *et al.* leveraged the alternating conjugate gradient method and particle swarm optimization algorithm for the joint UAV altitude and IRS phase shift optimization. In [14], Mei *et al.* investigated the RIS-assisted UAV communications and proposed two deep reinforcement learning (DRL) algorithms, where the 3D trajectory and RIS phase shifts were jointly optimized to minimize the UAV propulsion energy. Apart from the IRS-aided UAV communications, there are some notable works on the intelligent omni-surfaces (IOSs) assisted UAV communication, e.g., [15] and [16], which can further extend the wireless coverage and achieve omni-directional rate enhancement.

It is worth noting that all the above works perform the offline designs of UAV trajectory and reflection phase shifts in IRS-aided UAV networks, where all variables are determined prior to the flight. However, such an approach may suffer considerable performance loss for channels with non-negligible small-scale fading. This is because offline IRS phase shifts are designed based on the deterministic channel model, which cannot adapt to the instantaneous CSI along the UAV's flight. To tackle this challenge, Zhao *et al.* proposed a two-timescale beamforming for IRS in [17], where the long-term phase shifts are optimized via the statistical CSI and the short-term transmit beamforming is designed adaptive to the instantaneous CSI. For UAV-aided communications, You and Zhang proposed a hybrid offline-online design in [18], which determines the UAV path based on the statistical CSI in the offline phase, while adjusting its speed and scheduling based on the instantaneous CSI in the online phase.

Although plenty of research has combined UAV and IRS with offline design, the offline-online hybrid design for IRS-assisted UAV networks is not well investigated. Motivated by

Tianhao Wang, Xiaowei Pang and Nan Zhao are with the School of Information and Communication Engineering, Dalian University of Technology, Dalian 116024, China (email: nashifeng123@mail.dlut.edu.cn; xiaoweipang00@mail.dlut.edu.cn; zhaonan@dlut.edu.cn).

Mingqian Liu is with the State Key Laboratory of Integrated Service Networks, Xidian University Shaanxi, Xi'an 710071, China (e-mail: mqliu@mail.xidian.edu.cn).

Arumugam Nallanathan is with the Queen Mary University of London, E14NS London, U.K. (e-mail: a.nallanathan@qmul.ac.uk).

Xianbin Wang is with the Department of Electrical and Computer Engineering, Western University, London, ON N6A 3K7, Canada (e-mail: xianbin.wang@uwo.ca)

(Corresponding author: Nan Zhao)
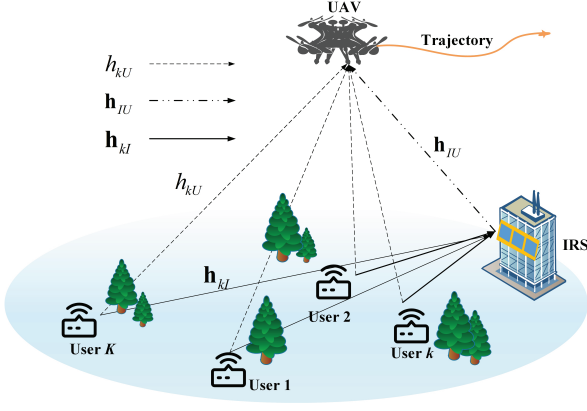
Fig. 1. IRS-assisted UAV uplink communication.

this, we propose an offline-online design to maximize the EE of IRS-aided UAV communication by jointly designing the trajectory, user scheduling and phase shifts. Specifically, we assume that the system only knows the statistical CSI prior to the flight to design the trajectory and user scheduling, while it can obtain the instantaneous CSI to readjust the phase shifts while flying. Numerical results demonstrate the effectiveness of the proposed online adjustment in leveraging the instantaneous CSI to improve the system performance, with low computational complexity.

II. SYSTEM MODEL

As shown in Fig. 1, we consider an uplink system where a rotary-wing UAV equipped with a single antenna is deployed to collect data from K single-antenna ground users with the aid of an IRS within a duration T. The set of K users is denoted by $\mathcal{K} = \{1, \ldots, K\}$. The horizontal coordinates of the kth user and the IRS are $\mathbf{L}_k = [x_k, y_k], \forall k$ and $\mathbf{L}_I = [x_I, y_I]$, respectively, and the altitudes of IRS and UAV are denoted by H_I and H_U, respectively. T is divided into N time slots with each equal to $\delta_t = T/N$, and the UAV's trajectory can be approximated as $\mathbf{q}[n] = [x[n], y[n]], n \in \mathcal{N} = \{1, \ldots, N\}$, with $\mathbf{q}_I$ and $\mathbf{q}_F$ denoting the UAV's initial and final horizontal locations, respectively. As a result, we have

$$\mathbf{q}[1] = \mathbf{q}_I, \|\mathbf{q}[N] - \mathbf{q}_F\|^2 \leq (V_m \delta_t)^2, \quad (1)$$

$$\|\mathbf{q}[n+1] - \mathbf{q}[n]\|^2 \leq (V_m \delta_t)^2, n = 1, \ldots N-1, \quad (2)$$

where V_m denotes the maximum speed of UAV.

Assume that the IRS is equipped with M reflecting elements, whose phase-shifting matrix in slot n is denoted by $\mathbf{\Theta}[n] = \text{diag}(e^{j\theta_1[n]}, \ldots, e^{j\theta_m[n]}, \ldots, e^{j\theta_M[n]}) \in \mathbb{C}^{M \times M}, \forall n$, where $\theta_m[n] \in [0, 2\pi)$ represents the phase shift incurred by the mth reflecting element. Let $\mathbf{h}_{kI}[n] \in \mathbb{C}^{M \times 1}$, $\mathbf{h}_{IU}[n] \in \mathbb{C}^{M \times 1}$ and $h_{kU}[n] \in \mathbb{C}^{1 \times 1}$ denote the channels from the kth user to the IRS, from the IRS to the UAV and from the kth user to the UAV, respectively. The composite channel for the kth user can be given by

$$h_k[n] = \mathbf{h}_{IU}^H[n]\mathbf{\Theta}[n]\mathbf{h}_{kI}[n] + h_{kU}[n], \forall k, \forall n. \quad (3)$$

To account for both the large-scale and small-scale fading, all these direct and reflecting links can be modeled by the Rician fading as

$$\mathbf{h}_{kI}[n] = \sqrt{\frac{\rho}{d_{kI}^{\beta_1}}} \left(\sqrt{\frac{K_1}{K_1+1}} \overline{\mathbf{h}}_{kI} + \sqrt{\frac{1}{K_1+1}} \widetilde{\mathbf{h}}_{kI}[n] \right), \quad (4)$$

$$\mathbf{h}_{IU}[n] = \sqrt{\frac{\rho}{d_{IU}[n]^{\beta_2}}} \left(\sqrt{\frac{K_2}{K_2+1}} \overline{\mathbf{h}}_{IU}[n] + \sqrt{\frac{1}{K_2+1}} \widetilde{\mathbf{h}}_{IU}[n] \right), (5)$$

$$h_{kU}[n] = \sqrt{\frac{\rho}{d_{kU}[n]^{\beta_3}}} \left(\sqrt{\frac{K_3}{K_3+1}} \overline{h}_{kU}[n] + \sqrt{\frac{1}{K_3+1}} \widetilde{h}_{kU}[n] \right), (6)$$

where ρ is the channel power gain at the reference distance, K_1, K_2 and K_3 are the Rician factors, and β_1, β_2 and β_3 denote the path-loss exponents. $d_{kI} = \sqrt{\|\mathbf{L}_k - \mathbf{L}_I\|^2 + H_I^2}$, $d_{UI}[n] = \sqrt{\|\mathbf{q}[n] - \mathbf{L}_I\|^2 + (H_U - H_I)^2}$ and $d_{kU}[n] = \sqrt{\|\mathbf{q}[n] - \mathbf{L}_k\|^2 + H_U^2}$ denote the distances from the IRS to the kth user, from the IRS to the UAV and from the kth user to the UAV, respectively. In addition, $\overline{\mathbf{h}}_{kI}$, $\overline{\mathbf{h}}_{IU}[n]$ and $\overline{h}_{kU}[n]$ denote the LoS components, while $\widetilde{\mathbf{h}}_{kI}[n]$, $\widetilde{\mathbf{h}}_{IU}[n]$ and $\widetilde{h}_{kU}[n]$ denote the non-LoS (NLoS) components, whose elements are independent and identically distributed complex Gaussian random variables with zero mean and unit variance. A uniform linear array (ULA) is considered for IRS. Thus, $\overline{\mathbf{h}}_{kI}$, $\overline{\mathbf{h}}_{IU}[n]$ and $\overline{h}_{kU}[n]$ are given by

$$\overline{\mathbf{h}}_{kI} = e^{-j\frac{2\pi}{\lambda}d_{kI}} \left[1, \ldots, e^{-j\frac{2\pi}{\lambda}\widetilde{d}(M-1)\sin\theta_{kI}\cos\phi_{kI}} \right]^T, \quad (7)$$

$$\overline{\mathbf{h}}_{IU}[n] = e^{-j\frac{2\pi}{\lambda}d_{IU}[n]} \left[1, \ldots, e^{-j\frac{2\pi}{\lambda}\widetilde{d}(M-1)\sin\theta_{IU}[n]\cos\phi_{IU}[n]} \right]^T, (8)$$

$$\overline{h}_{kU}[n] = e^{-j\frac{2\pi}{\lambda}d_{kU}[n]}, \quad (9)$$

where $\sin\theta_{kI}\cos\phi_{kI} = \frac{x_k - x_I}{d_{k,I}}$ and $\sin\theta_{IU}[n]\cos\phi_{IU}[n] = \frac{x_I - x_U[n]}{d_{IU}[n]}$. $\widetilde{d}$ is the element separation of IRS and λ is the carrier wavelength.

Consider that at most one user is served in each slot. Define a binary variable $\alpha_k[n]$ to illustrate the user scheduling, where the kth user is served when $\alpha_k[n] = 1$ and keeps silent otherwise. Thus, the user scheduling should satisfy

$$\alpha_k[n] \in \{0,1\}, \forall k \in \mathcal{K}, \forall n \in \mathcal{N}, \quad (10)$$

$$\sum_{k=1}^{K} \alpha_k[n] \leq 1, \forall n \in \mathcal{N}. \quad (11)$$

Hence, the achievable rate for the kth user in the nth time slot can be expressed as

$$R_k[n] = \alpha_k[n]B_W \log_2 \left(1 + P_t|h_k[n]|^2/\sigma^2 \right), \quad (12)$$

where B_W, P_t and σ^2 denote the channel bandwidth, the fixed transmit power and the additive white Gaussian noise power at the receiver, respectively. Note that $R_k[n]$ is a random variable since it involves the random NLoS components of $\widetilde{\mathbf{h}}_{kI}[n]$, $\widetilde{\mathbf{h}}_{IU}[n]$ and $\widetilde{h}_{kU}[n]$. We are interested in the expected achievable transmission rate $\mathbb{E}[R_k[n]]$, which is challenging

to obtain. By using the Jensen's inequality, the expected achievable rate $\mathbb{E}[R_k[n]]$ can be upper bounded by

$$\mathbb{E}[R_k[n]] \leq \alpha_k[n] B_W \log_2 \left(1 + P_t \mathbb{E}[|h_k[n]|^2]/\sigma^2\right) \\ \triangleq \bar{R}_k[n], \tag{13}$$

Similar to the proof in [Theorem 1, 11], $\mathbb{E}[|h_k[n]|^2]$ can be expressed as

$$\mathbb{E}[|h_k[n]|^2] = |h_{k,LOS}[n]|^2 + \\ \frac{\rho^2 d_{IU}^{-\beta_2}[n] d_{kI}^{-\beta_1}(K_1+K_2+1)M}{(K_1+1)(K_2+1)} + \frac{\rho d_{kU}^{-\beta_3}[n]}{K_3+1}, \tag{14}$$

with $h_{k,LOS}[n]$ denoted as

$$h_{k,LOS}[n] = \sqrt{\frac{\rho^2 d_{IU}^{-\beta_2}[n] d_{kI}^{-\beta_1} K_1 K_2}{(K_1+1)(K_2+1)}} \bar{\mathbf{h}}_{IU}^H[n] \mathbf{\Theta}[n] \bar{\mathbf{h}}_{kI} \\ + \sqrt{\frac{\rho d_{kU}^{-\beta_3}[n] K_3}{K_3+1}} \bar{h}_{kU}[n]. \tag{15}$$

III. PROBLEM FORMULATION

The system power includes the UAV's propulsion power, the users' transmit power and the circuit-related power. According to [3], the rotary-wing UAV's propulsion power in the nth time slot can be written as

$$P_{pro}[n] = P_0 \left(1 + \frac{3\Delta_n^2}{U_{tip}^2 \delta_t^2}\right) + \frac{1}{2} d_0 \rho S A \frac{\Delta_n^3}{\delta_t^3} + \tag{16}$$
$$P_i \left(\sqrt{1 + \frac{\Delta_n^4}{4v_0^4 \delta_t^4}} - \frac{\Delta_n^2}{2v_0^2 \delta_t^2}\right)^{\frac{1}{2}},$$

where $\Delta_n \triangleq \|\mathbf{q}[n+1] - \mathbf{q}[n]\|$. With (13) and (16), the EE can be approximately expressed as

$$EE = \frac{\sum\limits_{n=1}^{N} \sum\limits_{k=1}^{K} \bar{R}_k[n]}{\sum\limits_{n=1}^{N} P_{pro}[n] + \sum\limits_{n=1}^{N} \sum\limits_{k=1}^{K} \alpha_k[n] P_t + N \times P_C}, \tag{17}$$

where P_C is the fixed circuit-related power by UAV and IRS.

The objective is to maximize the EE by jointly optimizing the user scheduling, UAV trajectory and IRS phase-shifting matrix over N time slots, which can be formulated as

$$\max_{\mathbf{A}, \mathbf{Q}, \mathbf{\Theta}} \quad EE \tag{18a}$$
$$s.t. \ 0 \leq \theta_m[n] < 2\pi, \tag{18b}$$
$$\sum_{n=1}^{N} \bar{R}_k[n] \delta_t \geq B_k, \ \forall k \in \mathcal{K}, \tag{18c}$$
$$\sum_{n=1}^{N} (\alpha_k[n] P_t \delta_t) \leq E_k, \ \forall k \in \mathcal{K}, \tag{18d}$$
$$(1), (2), (10), (11). \tag{18e}$$

The problem (18) is an offline design by utilizing the statistical CSI and determining the optimal variables prior to the flight. However, the offline design may suffer from the performance loss due to the channel fading since the offline IRS phase shifts cannot adapt to the instantaneous CSI. In the next section, we will propose a joint offline-online scheme to tackle this problem.

IV. JOINT OFFLINE-ONLINE DESIGN

A. Offline Optimization

In the offline optimization, we aim at solving (18) by alternately optimizing $\mathbf{A}$ and $\mathbf{Q}$. We first obtain the closed-form solution to the IRS phase-shifting matrix with given $\mathbf{A}$ and $\mathbf{Q}$ according to the following proposition.

Proposition 1: For any given $\mathbf{A}$ and $\mathbf{Q}$, the mth optimal offline IRS phase shift to maximize $\bar{R}_k[n]$ can be given by

$$\theta_m^{off}[n] = \frac{2\pi}{\lambda} (d_{kI} - d_{IU}[n] - d_{kU}[n]) - \frac{2\pi (m-1) \tilde{d}}{\lambda} \times \\ (\sin \theta_{IU}[n] \cos \varphi_{IU}[n] - \sin \theta_{kI} \cos \varphi_{kI}). \tag{19}$$

Proof: According to [11], the closed-form solution to the phase shift of the mth element to optimize the composite channel $\mathbf{h}_{IU}^H[n] \mathbf{\Theta}[n] \mathbf{h}_{kI}[n] + h_{kU}[n]$ can be expressed as

$$\theta_m^*[n] = \arg(h_{kU}[n]) - \arg(h_{IU,m}^H[n]) - \arg(h_{kI,m}[n]), \tag{20}$$

where $h_{IU,m}^H[n]$ and $h_{kI,m}[n]$ denote the mth element of $\mathbf{h}_{IU}^H[n]$ and $\mathbf{h}_{kI}[n]$, respectively. Since we aim at deriving the offline phase shift $\theta_m^{off}[n]$ to maximize $\bar{R}_k[n]$ in (13), it is equivalent to maximize the first term of $\mathbb{E}[|h_k[n]|^2]$ in (14), i.e., $h_{k,LOS}[n]$. Thus, the mth optimal offline IRS phase shift can be given by

$$\theta_m^{off}[n] = \arg(\bar{h}_{kU}[n]) - \arg(\bar{h}_{IU,m}^H[n]) - \arg(\bar{h}_{kI,m}). \tag{21}$$

Substituting (7), (8) and (9) in (21), we arrive at (19). ∎

Based on Proposition 1, we can rewrite $\bar{R}_k[n]$ in (13) as

$$R_k^{off}[n] = \alpha_k[n] B_W \log_2 \left(1 + \frac{P_t}{\sigma^2} \left(d_{IU}^{-\beta_2}[n] CT_{k1}[n] \\ + d_{kU}^{-\beta_3}[n] \rho + d_{IU}^{\frac{-\beta_2}{2}}[n] d_{kU}^{\frac{-\beta_3}{2}}[n] CT_{k2}[n]\right)\right), \tag{22}$$

where $CT_{k1}[n]$ and $CT_{k2}[n]$ can be respectively given by

$$CT_{k1}[n] = \rho^2 d_{kI}^{-\beta_1} \frac{(K_1+K_2+1)M + K_1 K_2 M^2}{(K_1+1)(K_2+1)}, \tag{23}$$

$$CT_{k2}[n] = 2M \sqrt{\rho^3 d_{kI}^{-\beta_1} \frac{K_1 K_2 K_3}{(K_1+1)(K_2+1)(K_3+1)}}. \tag{24}$$

Therefore, the problem (18) can be simplified as

$$\max_{\mathbf{A}, \mathbf{Q}} \frac{\sum\limits_{n=1}^{N} \sum\limits_{k=1}^{K} R_k^{off}[n]}{\sum\limits_{n=1}^{N} P_{pro}[n] + \sum\limits_{n=1}^{N} \sum\limits_{k=1}^{K} \alpha_k[n] P_t + N \times P_C} \tag{25a}$$
$$s.t. \ \sum_{n=1}^{N} R_k^{off}[n] \delta_t \geq B_k, \forall k \in \mathcal{K}, \tag{25b}$$
$$(1), (2), (10), (11), (18d). \tag{25c}$$

In order to tackle the fractional objective of (25a), we transform it into a non-fractional form through the Dinkelbach's method. With the given Dinkelbach parameter $\eta_{(i)}$ in the ith Dinkelbach iteration, the problem (25) can be converted as

$$\max_{\mathbf{A}, \mathbf{Q}} \ \Phi(\mathbf{A}, \mathbf{Q}, \eta_{(i)}) \tag{26a}$$
$$s.t. \ (1), (2), (10), (11), (18d), (25b), \tag{26b}$$

where

$$\Phi(\mathbf{A}, \mathbf{Q}, \eta_{(i)}) = \sum_{n=1}^{N} \sum_{k=1}^{K} R_k^{off}[n] - \eta_{(i)} \sum_{n=1}^{N} \big(P_{pro}[n]$$
$$+ \sum_{k=1}^{K} \alpha_k[n] P_t + P_C \big). \tag{27}$$

In the following, (26) is decomposed into two subproblems by invoking the BCD and then alternately optimized.

1) User Scheduling Optimization: To tackle the binary variables, we relax $\mathbf{A}$ into continuous ones between 0 and 1. With the given $\mathbf{Q}$, the user scheduling can be written as

$$\max_{\mathbf{A}} \quad \Phi(\mathbf{A}, \mathbf{Q}, \eta_{(i)}) \tag{28a}$$
$$s.t. \ 0 \le \alpha_k[n] \le 1, \tag{28b}$$
$$(11), (18d), (25b). \tag{28c}$$

Since both the objective and constraints are linear with respect to $\mathbf{A}$, (28) is a standard linear programming. In addition, due to the relaxation of $\mathbf{A}$, the obtained solution should be reconstructed as binary ones by comparing with 0.5.

2) UAV Trajectory Optimization: For any given $\mathbf{A}$, the UAV trajectory optimization can be written as

$$\max_{\mathbf{Q}} \quad \Phi(\mathbf{A}, \mathbf{Q}, \eta_{(i)}) \tag{29a}$$
$$s.t. \ (1), (2), (25b). \tag{29b}$$

It is observed from (16) that the third term in $P_{pro}[n]$ is non-convex. As such, we introduce slack variables $A_p[n]$ as

$$A_p[n]^2 \ge \sqrt{1 + \frac{\Delta_n^4}{4v_0^4 \delta_t^4}} - \frac{\Delta_n^2}{2v_0^2 \delta_t^2}. \tag{30}$$

Therefore, $P_{pro}[n]$ can be rewritten as

$$P_{pro}^{A_p}[n] = P_0 \left(1 + \frac{3\Delta_n^2}{U_{tip}^2 \delta_t^2} \right) + \frac{1}{2} d_0 \rho S A \frac{\Delta_n^3}{\delta_t^3} + P_i A_p[n]. \tag{31}$$

To deal with the non-convex $R_k^{off}[n]$, we introduce auxiliary variables $x_{k1}[n]$, $y_{k1}[n]$ and $z_{k1}[n]$ to recast (29) as

$$\max_{\substack{\mathbf{Q}, A_p[n], z_{k1}[n] \\ x_{k1}[n], y_{k1}[n]}} \Phi_U(\mathbf{Q}, \eta_{(i)}) \tag{32a}$$

$$s.t. \ \sum_{n=1}^{N} \alpha_k[n] B_W \log_2 \Big(1 + \frac{P_t}{\sigma^2} \big(x_{k1}[n] CT_{k1}[n]$$
$$+ y_{k1}[n]\rho + z_{k1}[n] CT_{k2}[n] \big) \Big) \delta_t \ge B_k, \tag{32b}$$

$$\frac{1}{A_p[n]^2} \le A_p[n]^2 + \frac{\Delta_n^2}{v_0^2 \delta_t^2}, \tag{32c}$$

$$x_{k1}[n] \le d_{IU}^{-\beta_2}[n], \tag{32d}$$

$$y_{k1}[n] \le d_{kU}^{-\beta_3}[n], \tag{32e}$$

$$\frac{z_{k1}[n]^2}{y_{k1}[n]} \le x_{k1}[n], \tag{32f}$$

$$(1), (2), \tag{32g}$$

Algorithm 1 Iterative Algorithm for (25)

Input: Set the Dinkelbach iteration index $i = 0$, the Dinkelbach parameter $\eta_{(i)} = 0$ and the threshold $\Delta_1 > 0$.

1: **while** $\eta_{(i)} - \eta_{(i-1)} > \Delta_1$ **do**
2:     Set the BCD iteration index $t = 0$, the convergence threshold $\Delta_2 > 0$ and feasible points $\mathbf{A}^{(0)}$ and $\mathbf{Q}^{(0)}$.
3:     **while** $\Phi(\mathbf{A}^{(t)}, \mathbf{Q}^{(t)}, \eta_{(i)}) - \Phi(\mathbf{A}^{(t-1)}, \mathbf{Q}^{(t-1)}, \eta_{(i)}) > \Delta_2$ **do**
4:         Solve (28) via CVX and obtain $\mathbf{A}^{(t+1)}$;
5:         Solve (34) via CVX and obtain $\mathbf{Q}^{(t+1)}$;
6:         Calculate $\Phi(\mathbf{A}^{(t+1)}, \mathbf{Q}^{(t+1)}, \eta_{(i)})$;
7:         Update: $t = t + 1$;
8:     **end while**
9:     Set $\{\mathbf{A}^{(i+1)}, \mathbf{Q}^{(i+1)}\} = \{\mathbf{A}^{(t)}, \mathbf{Q}^{(t)}\}$.
10:     $\eta_{(i+1)} = \dfrac{\sum_{n=1}^{N} \sum_{k=1}^{K} \big(\bar{R}_k^{(i+1)}[n] \big)}{\sum_{n=1}^{N} P_{pro}^{(i+1)}[n] + \sum_{n=1}^{N} \sum_{k=1}^{K} \alpha_k^{(i+1)}[n] P_t + N \times P_C}$;
11:     Update: $i = i + 1$;
12: **end while**

Output: The final solution set $\{\mathbf{A}^*, \mathbf{Q}^*\} = \{\mathbf{A}^{(i)}, \mathbf{Q}^{(i)}\}$.

---

where

$$\Phi_U(\mathbf{Q}, \eta_{(i)}) = \sum_{n=1}^{N} \sum_{k=1}^{K} \alpha_k[n] B_W \log_2 \Big(1 + \frac{P_t}{\sigma^2} \big(x_{k1}[n] CT_{k1}[n] + y_{k1}[n]$$
$$\rho + z_{k1}[n] CT_{k2}[n] \big) \Big) - \eta_{(i)} \sum_{n=1}^{N} \Big(P_{pro}^{A_p}[n] + \sum_{k=1}^{K} \alpha_k[n] P_t + P_C \Big). \tag{33}$$

By replacing the right-hand side of (32c), (32d) and (32e) with their first-order Taylor expansions at the given feasible points $A_p^t[n]$ and $\mathbf{q}^t[n]$ in the tth BCD iteration, we have the constraints (35)-(37) shown at the top of the next page. Therefore, (32) can be converted as

$$\max_{\substack{\mathbf{Q}, A_p[n], z_{k1}[n] \\ x_{k1}[n], y_{k1}[n]}} \Phi_U(\mathbf{Q}, \eta_{(i)}) \tag{34a}$$

$$s.t. \ (1), (2), (32b), (32f), (35), (36), (37), \tag{34b}$$

which is convex and can be solved by CVX. The algorithm for solving (25) is summarized in Algorithm 1. In the inner layer, with the given Dinkelbach parameter $\eta_{(i)}$, the objective value of (26) is non-decreasing after each iteration as well as upper bounded by a finite value. In the outer layer, we gradually update the Dinkelbach parameter. Based on the convergence proof in [19], this Dinkelbach-based Algorithm is guaranteed to converge. In Step 4 and Step 5, the complexity for solving (28) and (34) are represented by $\mathcal{O}(KN)$ and $\mathcal{O}(3KN + 3N)^{3.5}$. Thus, the computational complexity can be given by $\mathcal{O}\left(N_D N_B (3KN + 3N)^{3.5} \right)$, where N_D and N_B denote the number of iterations for the Dinkelbach's method and BCD.

B. Online Optimization

During the UAV's flight, directly using the offline IRS phase shifts via the statistical CSI may suffer from the performance

$$\frac{1}{A_p^t[n]^2} \le A_p^t[n]^2 + 2A_p^t[n]\left(A_p[n] - A_p^t[n]\right) + \frac{1}{v_0^2\delta_t^2}\left(-\left\|\mathbf{q}^t[n+1] - \mathbf{q}^t[n]\right\|^2 + 2\left(\mathbf{q}^t[n+1] - \mathbf{q}^t[n]\right)^T\left(\mathbf{q}^t[n+1] - \mathbf{q}^t[n]\right)\right), \quad (35)$$

$$x_{k1}[n] \le \left(\left\|\mathbf{q}^t[n] - \mathbf{L}_I\right\|^2 + (h_U - h_I)^2\right)^{-\frac{\beta_2}{2}} - \frac{\beta_2}{2}\left(\left\|\mathbf{q}^t[n] - \mathbf{L}_I\right\|^2 + (h_U - h_I)^2\right)^{-\frac{\beta_2}{2}-1} \times \left(\left\|\mathbf{q}[n] - \mathbf{L}_I\right\|^2 - \left\|\mathbf{q}^t[n] - \mathbf{L}_I\right\|^2\right), \quad (36)$$

$$y_{k1}[n] \le \left(\left\|\mathbf{q}^t[n] - \mathbf{L}_k\right\|^2 + h_U{}^2\right)^{-\frac{\beta_3}{2}} - \frac{\beta_3}{2}\left(\left\|\mathbf{q}^t[n] - \mathbf{L}_k\right\|^2 + h_U{}^2\right)^{-\frac{\beta_3}{2}-1} \times \left(\left\|\mathbf{q}[n] - \mathbf{L}_k\right\|^2 - \left\|\mathbf{q}^t[n] - \mathbf{L}_k\right\|^2\right). \quad (37)$$

loss due to the varying instantaneous CSI. To further improve the performance, we design the online policy that can adjust IRS's phase shifts to reach the signal alignment of direct and reflecting links and maximize the composite channel response $h_k[n]$ based on the instantaneous CSI during the flight such that the received signal strength can be maximized in real time. We assume that the perfect CSI is available to provide a theoretical performance upper bound. According to Proposition 1, the mth optimal online IRS phase shift in the nth slot can be given by

$$\theta_m^{on}[n] = \arg\left(h_{kU}[n]\right) - \arg\left(h_{IU,m}^H[n]\right) - \arg\left(h_{kI,m}[n]\right). \quad (38)$$

Thus, we can adopt the online phase shift $\theta_m^{on}[n]$ according to the closed-form solution in (38) with low computational complexity to replace the offline one $\theta_m^{off}[n]$ in (21) to achieve better performance.

Based on Algorithm 1 and (38), the joint offline-online design can be briefly summarized as follows. In the offline design, the initial UAV trajectory and user scheduling can be designed by Algorithm 1 and then performed by the UAV. Then, in the online design, the UAV can acquire the instantaneous CSI during its flight, based on which, the optimal online IRS phase shifts can be calculated accordingly. Therefore, combining the statistical CSI based trajectory and scheduling and the instantaneous CSI based phase shifts can contribute to a better performance.

V. NUMERICAL RESULTS

We present numerical results to verify the effectiveness of the proposed scheme. The UAV is assumed to fly from $\mathbf{q_I} = [-300, 150]$ m towards $\mathbf{q_F} = [300, 150]$ m within $T = 60$ s with $V_m = 20$ m/s. Set $\delta_t = 1$ s, $H_U = 100$ m and $H_I = 20$ m. $K = 3$ users are considered, which are located on the ground at $\mathbf{L_1} = [-20, 90]$ m, $\mathbf{L_2} = [0, 50]$ m and $\mathbf{L_3} = [30, 100]$ m with $P_t = 0.1$ W. The IRS is located at $[0,0]$ m. Other parameters are set as $\rho = -40$ dB, $\sigma^2 = -90$ dBm, $\widetilde{d}/\lambda = 0.25$, $\beta_1 = 2.4$, $\beta_2 = 2.2$, $\beta_3 = 3.5$, $K_1 = 3$, $K_2 = 10$, $K_3 = 10$ and $B_W = 360$ kHz.

We compare the following benchmarks: a) Conventional Scheme, which adopts the offline policy based on the outdated CSI with no online adjustment. b) Offline-NoOnline Scheme, which obtains $\mathbf{A}$, $\mathbf{Q}$ and $\mathbf{\Theta}$ based on the statistical CSI by Algorithm 1 with no online adjustment. c) Random IRS Scheme, where $\mathbf{\Theta}$ is randomly generated in each slot. d) No IRS Scheme, without deploying IRS. The proposed scheme is named as Offline-Online Scheme. Fig. 2 plots the UAV trajectories of the proposed scheme and No IRS scheme, with $B = 5$ bit/Hz and $E = 2$ J. We can see that the UAV hovers
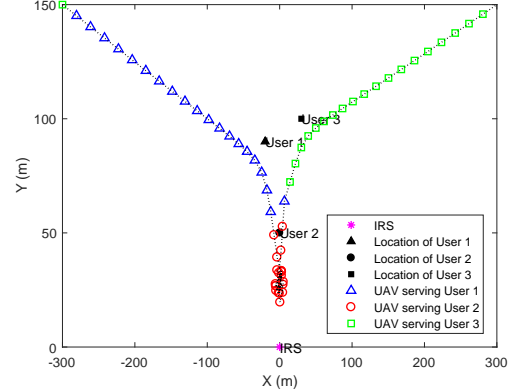
(a) Proposed Scheme
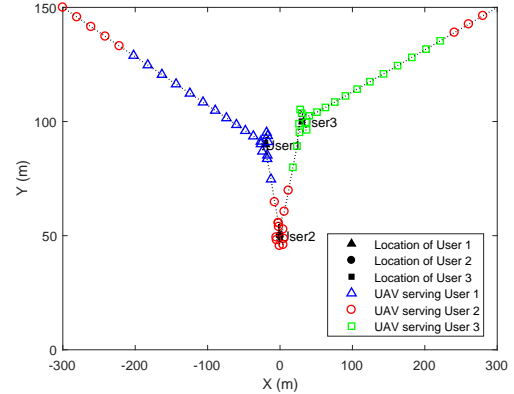
(b) No IRS Scheme

Fig. 2. Trajectories of UAV of the proposed scheme and the No IRS scheme.

around each user for a while in both schemes. This is because the UAV needs to balance the throughput and the propulsion energy. The most striking difference is that the UAV hovers between User 2 and IRS for a long time in Fig. 2(a) while it hovers sequentially above the three users in Fig. 2(b) to establish the best channels for them. This is because the IRS can reconfigure the propagation environment, and its nearby user (i.e., User 2) can attain the optimal composite channel with comparable direct and reflecting channels.

To further show the effectiveness of IRS, we plot the EE versus the number of IRS reflecting elements in Fig. 3. It shows that the EE of the proposed scheme outperforms those of the Offline-NoOnline scheme and the Conventional scheme. The main reason is that in the Offline-NoOnline scheme and the Conventional scheme, the phase shifts are obtained according to the outdated CSI, which results in nonnegligible
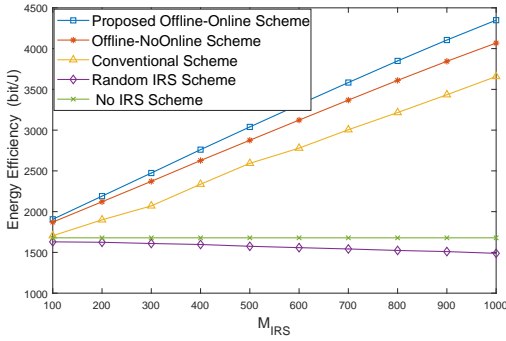
Fig. 3. Energy efficiency versus the number of IRS reflecting elements.
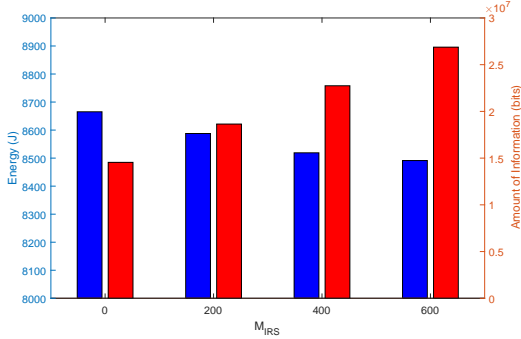
Fig. 4. Propulsion energy and amount of information versus the number of IRS reflecting elements.

performance loss. In contrast, the proposed scheme can adjust the phase shifts in an online manner to fully improve its passive beamforming gain. Meanwhile, more reflecting elements can provide higher passive beamforming gain, making the online adjustment more effective. Compared with the No IRS scheme and the Random IRS scheme, the EE of the proposed scheme is significantly higher than these two benchmarks and the gap increases with M_{IRS}.

Fig. 4 presents the impact of introducing IRS on the UAV propulsion energy and amount of information, Note that $M_{IRS} = 0$ corresponds to No IRS scheme. We can see that No IRS scheme consumes the highest propulsion energy but transmits the least amount of information. As M_{IRS} increases, the propulsion energy decreases while the amount of information significantly increases. This phenomenon can be attributed to the ability of the IRS to manipulate the wireless channel by aligning the phase of reflecting link with that of direct link to achieve coherent signal combining. Additionally, UAV hovers around users with favorable channel conditions for the maximum possible duration at the speed with minimum propulsion power, thereby reducing propulsion energy. Thus, introducing IRS into UAV communication can enhance network throughput while reducing the UAV's energy consumption. As a result, the EE increases with the number of IRS reflecting elements.

VI. CONCLUSION

In this correspondence, we have proposed an offline-online design of the UAV trajectory, user scheduling and IRS's phase shifts for IRS-aided UAV communications to maximize the EE. Specifically, the offline optimization can determine the UAV trajectory and user scheduling via the Dinkelbach's method and BCD, while the online optimization can adaptively tune IRS's phase shifts according to the closed-form solution during the flight. Simulation results show that the EE can be significantly improved by the offline-online design compared to benchmarks.

REFERENCES

[1] Y. Zeng, R. Zhang, and T. J. Lim, "Wireless communications with unmanned aerial vehicles: opportunities and challenges," *IEEE Commun. Mag.*, vol. 54, no. 5, pp. 36–42, May 2016.
[2] X. Jiang, M. Sheng, N. Zhao, C. Xing, W. Lu, and X. Wang, "Green UAV communications for 6G: A survey," *Chin. J. Aeronaut.*, vol. 35, no. 9, pp. 19–34, Sept. 2022.
[3] Y. Zeng, J. Xu, and R. Zhang, "Energy minimization for wireless communication with rotary-wing UAV," *IEEE Trans. Wireless Commun.*, vol. 18, no. 4, pp. 2329–2345, Apr. 2019.
[4] B. Duo, Q. Wu, X. Yuan, and R. Zhang, "Energy efficiency maximization for full-duplex UAV secrecy communication," *IEEE Trans. Veh. Technol.*, vol. 69, no. 4, pp. 4590–4595, Apr. 2020.
[5] Q. Wu and R. Zhang, "Intelligent reflecting surface enhanced wireless network via joint active and passive beamforming," *IEEE Trans. Wireless Commun.*, vol. 18, no. 11, pp. 5394–5409, Nov. 2019.
[6] Y. Xu, T. Zhang, Y. Liu, D. Yang, L. Xiao, and M. Tao, "Computation capacity enhancement by joint UAV and RIS design in IoT," *IEEE Internet Things J*, vol. 9, no. 20, pp. 20590–20603, Oct. 2022.
[7] Y. Byun, H. Kim, S. Kim, and B. Shim, "Channel estimation and phase shift control for UAV-carried RIS communication systems," *IEEE Trans. Veh. Technol.*, to appear.
[8] X. Pang, M. Sheng, N. Zhao, J. Tang, D. Niyato, and K.-K. Wong, "When UAV meets IRS: Expanding air-ground networks via passive reflection," *IEEE Wireless Commun.*, vol. 28, no. 5, pp. 164–170, Oct. 2021.
[9] Z. Zhai, X. Dai, B. Duo, X. Wang, and X. Yuan, "Energy-efficient UAV-mounted RIS assisted mobile edge computing," *IEEE Wireless Commun. Lett.*, vol. 11, no. 12, pp. 2507–2511, Dec. 2022.
[10] S. Li, B. Duo, M. D. Renzo, M. Tao, and X. Yuan, "Robust secure UAV communications with the aid of reconfigurable intelligent surfaces," *IEEE Trans. Wireless Commun.*, vol. 20, no. 10, pp. 6402–6417, Oct. 2021.
[11] M. Hua, L. Yang, Q. Wu, C. Pan, C. Li, and A. L. Swindlehurst, "UAV-assisted intelligent reflecting surface symbiotic radio system," *IEEE Trans. Wireless Commun.*, vol. 20, no. 9, pp. 5769–5785, Sept. 2021.
[12] X. Mu, Y. Liu, L. Guo, J. Lin, and H. V. Poor, "Intelligent reflecting surface enhanced Multi-UAV NOMA networks," *IEEE J. Sel. Areas Commun.*, vol. 39, no. 10, pp. 3051–3066, Oct. 2021.
[13] M. Misbah, Z. Kaleem, W. Khalid, C. Yuen, and A. Jamalipour, "Phase and 3D Placement Optimization for Rate Enhancement in RIS-Assisted UAV Networks," *IEEE Wireless Commun. Lett.*, pp. 1–1, 2023.
[14] H. Mei, K. Yang, Q. Liu, and K. Wang, "3D-Trajectory and Phase-Shift Design for RIS-Assisted UAV Systems Using Deep Reinforcement Learning," *IEEE Trans. Veh. Technol.*, vol. 71, no. 3, pp. 3020–3029, 2022.
[15] Y. Lei, Y. Liu, Q. Wu, X. Yuan, J. Ning, and B. Duo, "Enhancing UAV-Enabled Communications via Multiple Intelligent Omni-Surfaces," *IEEE Commun. Lett.*, vol. 27, no. 2, pp. 655–660, 2023.
[16] Q. Zhang, Y. Zhao, H. Li, S. Hou, and Z. Song, "Joint Optimization of STAR-RIS Assisted UAV Communication Systems," *IEEE Wireless Commun. Lett.*, vol. 11, no. 11, pp. 2390–2394, 2022.
[17] M.-M. Zhao, Q. Wu, M.-J. Zhao, and R. Zhang, "Intelligent reflecting surface enhanced wireless networks: Two-timescale beamforming optimization," *IEEE Trans. Wireless Commun.*, vol. 20, no. 1, pp. 2–17, Jan. 2021.
[18] C. You and R. Zhang, "Hybrid offline-online design for UAV-enabled data harvesting in probabilistic LoS channels," *IEEE Trans. Wireless Commun.*, vol. 19, no. 6, pp. 3753–3768, Jun. 2020.
[19] W. Dinkelbach, "On nonlinear fractional programming," *Manage. Sci*, vol. 13, no. 7, pp. 492–498, 1967.